DYNAMICS MODELING AND VIBRATION SUPPRESSION OF HIGH-SPEED MAGNETICALLY SUSPENDED ROTOR CONDERING FIRST-ORDER ELASTIC NATURAL VIBRATION

Wei Tong **Fang Jiancheng**
The 5th Unit, Beijing University of Aeronautics and Astronautics, Beijing, P.R.China, 100083
weitong3000@sina.com

ABSTRACT

In magnetically suspended rotor of control moment gyro (CMG), for the sake of raising the ratio of rotary inertia to rotor mass, the rotor is usually designed to have I-shaped-side-view construction, which weakens conjunction between disk and axis of rotor and reduces the frequency of first-order elastic natural vibration (ENV) characterized as relative bending between disk and axis. If this frequency is covered by control system bandwidth of active magnetic bearing (AMB), ENV becomes unstable. ENV can be depressed by inserting notch filter into AMB controller, and depression effects greatly depend on center frequency of notch filter, f_{c1}. In order to select optimized f_{c1} by means of simulation, dynamic model of rotor and a method to evaluate introduced parameters, k_k and k_v were presented considering ENV mode. In whole rotational speed range this model was utilized to simulate ENV depression, and effects associated with different f_{c1} were discussed. Corresponding experiments were performed in the magnetic bearing-rotor system of CMG developed by Beijing University of Aeronautics and Astronautics. ENV amplitude was depressed to 0.1% compared to original, which verified ENV model and confirmed simulation results.

INTRODUCTION

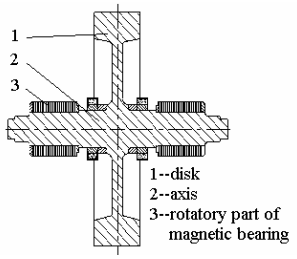

Figure 1: I-shaped side view of CMG rotor

Control moment gyro (CMG), consisting of high-speed rotor system and gimbal system, is the key attitude-control actuator for large spacecrafts. The rotor system serves as the main part of CMG, and for the sake of high speed and long life, active magnetic bearing (AMB) superior in properties of non-contact and non-friction is adopted as the most effective solution[1]. Furthermore, in order to maximize rotatory inertia without increasing rotor mass, rotor disk must be configured to distribute its majority of mass at rim, and thus has I-shaped side view (Figure 1). However, this construction weakens conjunction between disk and axis of rotor, and so reduces the frequency of first-order elastic natural vibration (ENV) characterized as relative bending between disk and axis. This frequency is lower than bandwidth of AMB control system due to rotor's high-speed property, therefore ENV mode becomes unstable and CMG rotor keeps oscillating violently.

A CMG based on AMB supported rotor is developed by Beijing University of Aeronautics and Astronautics (BUAA). The AMB control system consists of displacement sensors, PID controller, amplifier, electromagnets and rotor. Rate speed of rotor is 20000r/min and system bandwidth 4kHz. The above mentioned ENV signal and relevant FFT (fast Fourier transformation) of non-rotation rotor shaft end displacement are shown in figure 2, where rotor behavior contains high and low frequency sections. The higher one is the unstable ENV at 1140Hz and in 1.25dB (in the oscilloscope 0dB is corresponding to peak-to-peak 2.82 volts of sine wave, which indicates $35\mu m$ of rotor vibration in same manner). This ENV frequency of rotor without depression is named as original frequency, f_{p1}. The low frequency section is excited by high one, which causes rotor to impact touchdown bearing violently. Therefore, ENV must be depressed for system stability.

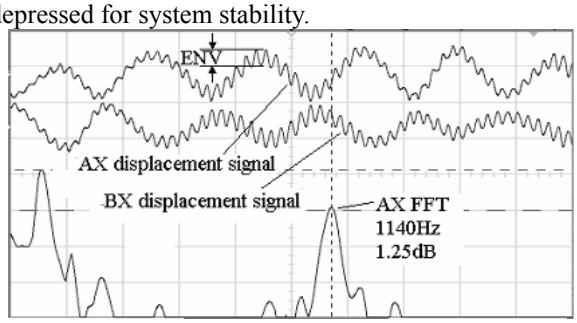

Figure2: Shaft end displacement and FFT of non-rotation rotor without depression method

AMB also has good qualities in vibration suppression, which can be achieved by inserting notch filter into AMB controller[2]. Both reference [2] and [3] adopted notch filters, whose center frequency varies along rotational speed, to eliminate oscillation caused by rotor unbalance. However, differing from unbalance vibration, ENV only changes within a narrow range, hereby notch filters can be designed with fixed center frequency for the sake of system simplicity. In order to

* This project is supported by Hi-tech Research and Development Program of China.

select optimized f_{c1} by means of simulation, and to ensure ENV stability within rotational speed range (i.e. from stationary to rate speed), dynamic model considering ENV mode should be set up. Usually, elastic structure motion can be described appropriately by discrete points within the structure when modeling[4]. Finite Element Method (FEM) was used to model continuously elastic body considering several orders of elastic modes simultaneously[5]. Multi-body model, another simplified description, deals with multi-rigid body with elastic connection which can be represented as spring-dashpot exhibiting stiffness and damping[6,7]. This spring-dashpot substitution also fits for continuously elastic body if only first-order elastic vibration mode is considered, Jeffcott rotor for example[8,9].

Multi-body method was utilized to model CMG rotor with ENV mode and a method to evaluate introduced parameters was presented in this paper. Then within rotational speed range ENV stability referring to different center frequency was simulated based on the model, and experimental results were presented. In the end were conclusions of this paper.

DYNAMICS MODELING OF ROTOR CONDERING ENV

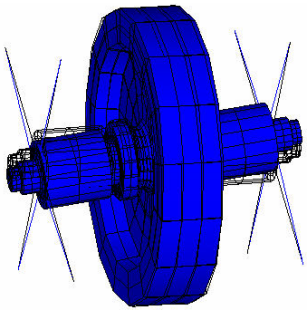

Figure3: ANSYS result about ENV mode

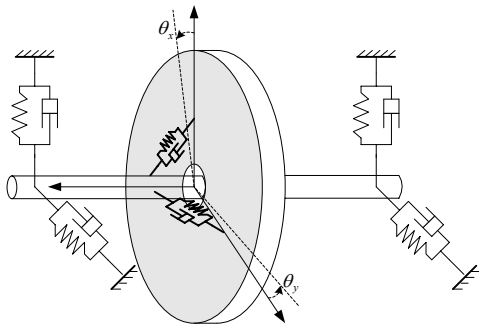

Figure 4: mechanic model of CMG rotor considering ENV

Calculation results according to ANSYS indicate that the first-order elastic vibration is characterized as the relative bending between disk and axis (figure 3), caused by finite intension in disk-axis conjunction compared to ideal rigid rotor. Consequently, the CMG rotor can be regarded as a two-body structure consisting of rigid disk and rigid axis with elastic conjunction. In figure 4, rigid disk and axis are connected by two angular spring-dashpots, which enables disk and axis to swing relatively in 2 DOFs (dimensions of freedom), but without translations and spin. Assuming disk rotates θ_x and θ_y about axis x and y respectively (corresponding to broken line in figure 4) and the axis keeps static, restoring moment imposed in the disk can be expressed as:

$$\begin{cases} p'_x = -k_k\theta_x - k_v\dot{\theta}_x \\ p'_y = -k_k\theta_y - k_v\dot{\theta}_y \end{cases} \tag{1}$$

where k_k(Nm/rad) is the stiffness of spring in rotational DOF, and k_v(Nms/rad) the damping.

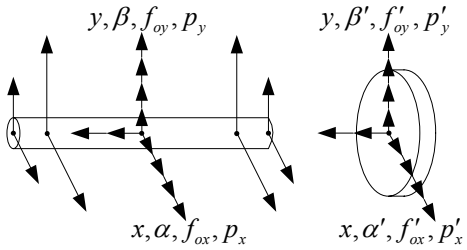

Figure 5: force diagrams of the axis and the disk

Using mechanic model above, force conditions of the axis and the disk are analyzed respectively in figure 5, where both ends of the rotor are symmetric about rotor center, and *oxyz* is rotor coordinate. The magnetic bearings lying in point A and B satisfy $|OA| = |OB| = l_m$, and displacement sensors in C and D satisfy $|OC| = |OD| = l_s$. All the vectors are shown as follows:

f_{ax}, f_{bx}, f_{ay}, f_{by} -- magnetic bearing forces

f_{ox}, f_{oy} -- forces of the disk to the axis

p_x, p_y -- moments of the disk to the axis

f'_{ox}, f'_{oy} -- forces of the axis to the disk

p'_x, p'_y -- moments of the axis to the disk

α, β -- angular displacements of the axis

α', β' -- angular displacements of the disk

H_1, H_2 -- angular momentums of the axis and the disk respectively

According to figure 5, kinetic equations of axis are:

$$\begin{cases} m_1\ddot{x} = f_{ax} + f_{bx} + f_{ox} \\ J_{1e}\ddot{\beta} - H_1\dot{\alpha} = (f_{ax} - f_{bx})l_m + p_y \\ m_1\ddot{y} = f_{ay} + f_{by} + f_{oy} \\ J_{1e}\ddot{\alpha} + H_1\dot{\beta} = (-f_{ay} + f_{by})l_m + p_x \end{cases} \tag{2}$$

where m_1, J_{1e} are mass and equator moment of inertia of axis respectively. And kinetic equation of disk is:

$$\begin{cases} m_2\ddot{x} = f'_{ox} \\ J_{2e}\ddot{\beta}' - H_2\dot{\alpha}' = p'_y \\ m_2\ddot{y} = f'_{oy} \\ J_{2e}\ddot{\alpha}' + H_2\dot{\beta}' = p'_x \end{cases} \tag{3}$$

where m_2, J_{2e} are mass and equator moment of inertia of disk respectively.

The first auxiliary equation is obtained according to equation (1):

$$\begin{cases} p'_x = k_k(\alpha-\alpha') + k_v(\dot\alpha-\dot\alpha') \\ p'_y = k_k(\beta-\beta') + k_v(\dot\beta-\dot\beta') \end{cases} \tag{4}$$

And according to Newton's third law, we have the second auxiliary equation:

$$\begin{cases} f_{ox} = -f'_{ox} \\ f_{oy} = -f'_{oy} \\ p_x = -p'_x \\ p_y = -p'_y \end{cases} \tag{5}$$

Let $m = m_1 + m_2$ as the mass of the whole rotor, and then incorporate equation (4) and (5) into equation (2) and (3), the rotor dynamic model considering ENV mode is:

$$\begin{cases} m\ddot x = f_{ax} + f_{bx} \\ m\ddot y = f_{ay} + f_{by} \\ J_{1e}\ddot\alpha + H_1\dot\beta + k_k(\alpha-\alpha') + k_v(\dot\alpha-\dot\alpha') = (-f_{ay}+f_{by})l_m \\ J_{1e}\ddot\beta - H_1\dot\alpha + k_k(\beta-\beta') + k_v(\dot\beta-\dot\beta') = (f_{ax}-f_{bx})l_m \\ J_{2e}\ddot\alpha' + H_2\dot\beta' - k_k(\alpha-\alpha') - k_v(\dot\alpha-\dot\alpha') = 0 \\ J_{2e}\ddot\beta' - H_2\dot\alpha' - k_k(\beta-\beta') - k_v(\dot\beta-\dot\beta') = 0 \end{cases} \tag{6}$$

Here if k_k tends to be infinite, the model will regress to gyroscopic technology equation due to $\alpha=\alpha'$ and $\beta=\beta'$. Therefore, the new model considering ENV mode is an extension from rigid rotor model, where only rigid modes of precession and nutation are included.

From equation (6), The state vector X can be defined as $\begin{bmatrix} x & \beta & y & -\alpha & \dot x & \dot\beta & \dot y & -\dot\alpha & \beta' & -\alpha' & \dot\beta' & -\dot\alpha' \end{bmatrix}^T$. Select magnetic bearing force $f_m = \begin{bmatrix} f_{ax} & f_{bx} & f_{ay} & f_{by} \end{bmatrix}^T$ as input vector, and sensor coordinates $q_s = \begin{bmatrix} x_{as} & x_{bs} & y_{as} & y_{bs} \end{bmatrix}^T$ the output vector, then the plant matrices of state equation are:

$A=$

$$\begin{bmatrix}
0 & 0 & 0 & 0 & 1 & 0 & 0 & 0 & 0 & 0 & 0 & 0 \\
0 & 0 & 0 & 0 & 0 & 1 & 0 & 0 & 0 & 0 & 0 & 0 \\
0 & 0 & 0 & 0 & 0 & 0 & 1 & 0 & 0 & 0 & 0 & 0 \\
0 & 0 & 0 & 0 & 0 & 0 & 0 & 1 & 0 & 0 & 0 & 0 \\
0 & 0 & 0 & 0 & 0 & 0 & 0 & 0 & 0 & 0 & 0 & 0 \\
0 & -\frac{k_k}{J_{1e}} & 0 & 0 & 0 & -\frac{k_v}{J_{1e}} & 0 & -\frac{H_1}{J_{1e}} & \frac{k_k}{J_{1e}} & 0 & \frac{k_v}{J_{1e}} & 0 \\
0 & 0 & 0 & 0 & 0 & 0 & 0 & 0 & 0 & 0 & 0 & 0 \\
0 & 0 & 0 & -\frac{k_k}{J_{1e}} & 0 & \frac{H_1}{J_{1e}} & 0 & -\frac{k_v}{J_{1e}} & 0 & \frac{k_k}{J_{1e}} & 0 & \frac{k_v}{J_{1e}} \\
0 & 0 & 0 & 0 & 0 & 0 & 0 & 0 & 0 & 0 & 1 & 0 \\
0 & 0 & 0 & 0 & 0 & 0 & 0 & 0 & 0 & 0 & 0 & 1 \\
0 & \frac{k_k}{J_{2e}} & 0 & 0 & 0 & \frac{k_v}{J_{2e}} & 0 & 0 & -\frac{k_k}{J_{2e}} & 0 & -\frac{k_v}{J_{2e}} & -\frac{H_2}{J_{2e}} \\
0 & 0 & 0 & \frac{k_k}{J_{2e}} & 0 & 0 & 0 & \frac{k_v}{J_{2e}} & 0 & -\frac{k_k}{J_{2e}} & \frac{H_2}{J_{2e}} & -\frac{k_v}{J_{2e}}
\end{bmatrix}$$

$$B = \begin{bmatrix}
 & & 0_{4\times4} & \\
1/m & 1/m & 0 & 0 \\
l_m/J_{1e} & -l_m/J_{1e} & 0 & 0 \\
0 & 0 & 1/m & 1/m \\
0 & 0 & l_m/J_{1e} & -l_m/J_{1e} \\
 & & 0_{4\times4} &
\end{bmatrix},$$

$$C = \begin{bmatrix}
1 & l_s & 0 & 0 & 0 & 0 & 0 & 0 & 0 & 0 & 0 & 0 \\
1 & -l_s & 0 & 0 & 0 & 0 & 0 & 0 & 0 & 0 & 0 & 0 \\
0 & 0 & 1 & l_s & 0 & 0 & 0 & 0 & 0 & 0 & 0 & 0 \\
0 & 0 & 1 & -l_s & 0 & 0 & 0 & 0 & 0 & 0 & 0 & 0
\end{bmatrix}.$$

For the sake of simulating based on ENV model, the new parameters, k_k and k_v, must be obtained. However, they are impossible to be measured directly and thus a parameter evaluation method is presented.

PARAMETERS EVALUATION METHOD

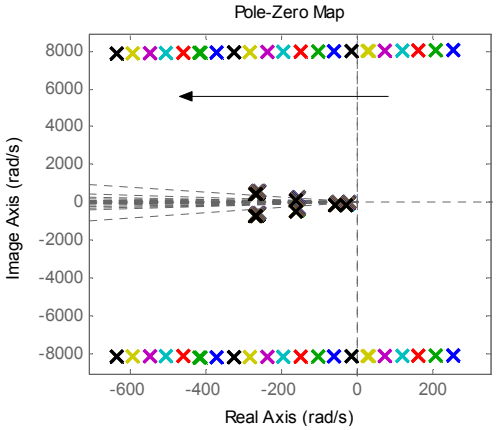

Figure 6: ENV poles locus when k_v changes from 0 to 20Nms/rad and k_k=700000Nm/rad. Rotor speed 0r/min. The arrow denotes step-up direction of k_v.

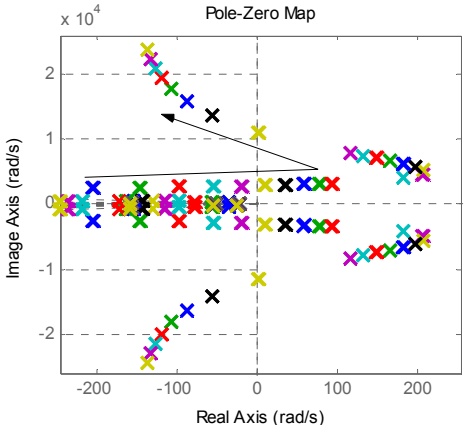

Figure 7: ENV poles locus when k_k changes from 7000 to 6300000Nm/rad and k_v=3Nms/rad. Rotor speed 0r/min. The arrow denotes k_k step-up direction.

ENV poles locus depending on various k_k and k_v when rotor is in static (rotor speed 0r/min) are shown in figure 6 and figure 7 respectively, where imaginary parts of poles represent ENV frequency. It can be seen that vibration frequency is primarily determined by k_k only

(increases with k_k), so k_k can be evaluated to be 540000Nm/rad according to figure 7, which is corresponding to the measured f_1 (equals to 1140Hz) in figure 2.

It can also be seen that k_v only influences mode stability according to figure 6, the larger k_v the better stability, so k_v can be evaluated through examining ENV stability. One grade of notch filter was introduced to stabilize AMB system, and stability margin depends on center frequency of notch filter, f_{c1}. Firstly, experiments in CMG indicated that ENV was stable when f_{c1} changes from 1046Hz to 1120Hz. Secondly, ENV poles locus with different f_{c1} and k_v was simulated (figure 8), which revealed that when k_v is 0.8Nms/rad, stable field of f_{c1}, from 1040Hz to 1150Hz, is close to experimental result especially.

General speaking, that k_k=540000Nm/rad and k_v =0.8Nms/rad are the final evaluated results.

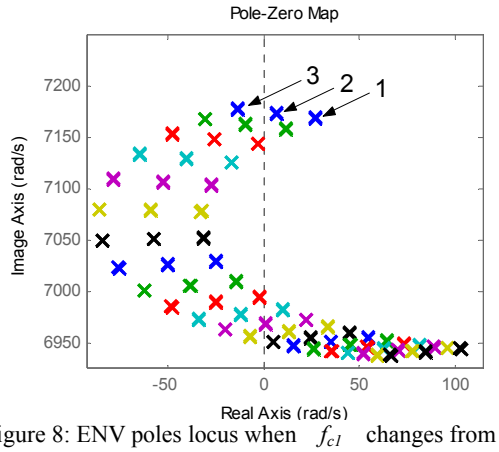

Figure 8: ENV poles locus when f_{cl} changes from 1040 to 1240Hz with step of 10Hz. k_k =540000Nm/rad and rotor speed 0prm. Locus 1—k_v is 0.4Nms/rad, locus 2—k_v 0.8 Nms/rad, locus 3—k_v 1.2 Nms/rad

ENV SUPPRESSION BY INSERTING NOTCH FILTER INTO AMB CONTROLLER

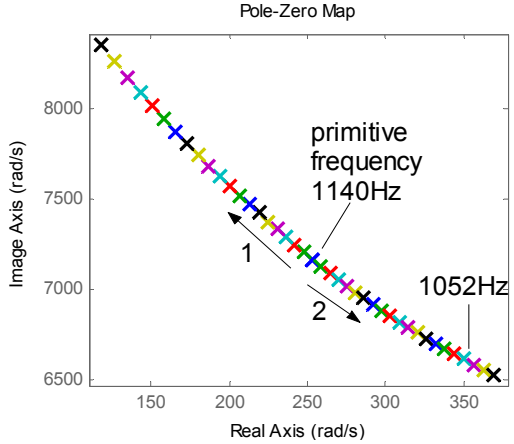

Figure 9: ENV poles locus without depression when rotational speed changes from stationary to 24000r/min with step of 1200r/min. The arrows denote speed ascending directions.

Base on the above model, ENV of magnetically suspended rotor without depression method is not stable within rotational speed range, relevant poles locus being showed in figure 9. When the rotor speed ascends from stationary, the poles locus of ENV turns into two branches, which starts from original frequency and goes upward and downward respectively. Obviously, Amplitude, stability and frequency of ENV are all determined by the branch with the least damping, which is defined as flag branch, and its frequency the flag frequency, f_1. Since flag branch is the descending one in figure 9, ENV without depression tends to decrease its frequency and shrink its stability owing to rotational speed ascending.

The adopted notch filter is showed in figure 10. Its simplified second-order transfer function can be expressed as following if neglecting real doublet:

$$G_{nf}(s) = \frac{s^2 + \omega_1^2}{s^2 + \dfrac{\omega_2}{Q/(1-k)}s + \omega_2^2} \qquad (7)$$

where $\omega_1 = 2\pi f_{c1} = \dfrac{1}{C\sqrt{3R_1R_2}}$, f_{c1} is center frequency, Q the quality factor of passive notch filter, and ω_2 the other transition frequency which is a bit larger than ω_1. To increase trap depth, two grades of notch filters are connected in series before inserting into AMB controller.

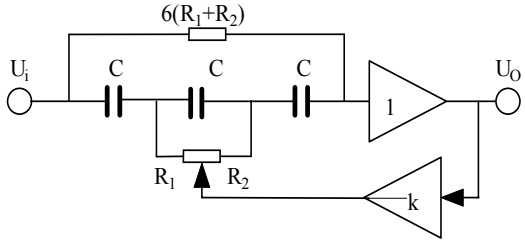

Figure 10: diagram of a notch filter

ENV suppression must ensure stability within the whole rotational speed range, and center frequency f_{c1} is one of the most important parameters of notch filter referring to depression effect. The ENV poles loci associated with f_{c1} around f_{p1} (original frequency) are supplied in figure11. It is found that with depression method, ENV also tends to be unstable when rotational speed grows. Since two grades of notch filters are employed, ENV loci increase to ten branches, but only branch 2 or 4 are possible to be flag branch, which depends on f_{c1} position relative to f_{p1}. From figure 11, depression effects determined by different f_{c1} are summarized in table 1. According to table 1, (1) ENV will become unstable if f_{c1} is far away from f_{p1} excessively; (2) the flag branch of ENV tends to lie in branch 2 and f_1 ascends with rotational speed if f_{c1} is smaller than f_{p1}, and ENV with higher f_{c1} shows reversal properties; (3) ENV is more stable if f_{c1} is smaller than f_{p1} compared to reversion. Therefore, the optimized f_{c1} which ensures stability within whole speed range must be a bit lower than f_{p1}, which is showed in the third situation in table 1.

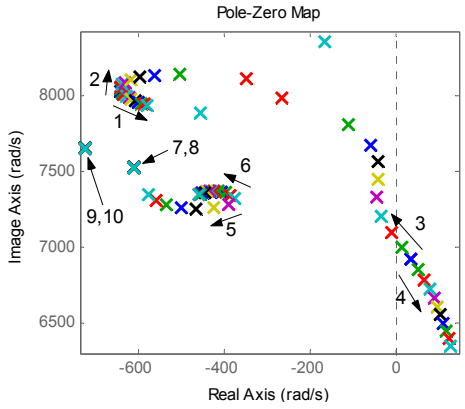

(11a) f_{c1}=1190Hz

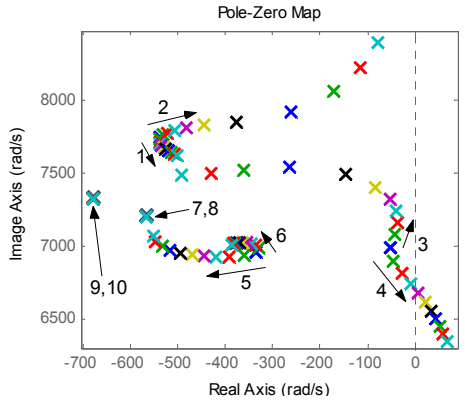

(11b) f_{c1}=1140Hz

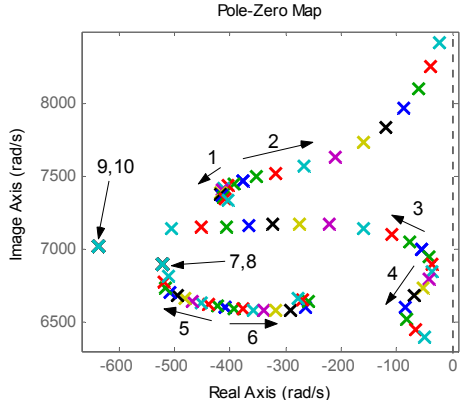

(11c) f_{c1}=1090Hz

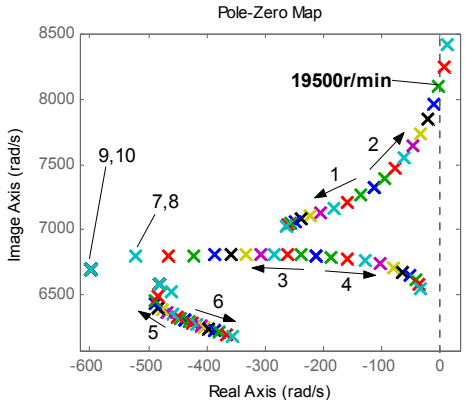

(11d) f_{c1}=1040Hz

Figure 11: ENV pole-zeros locus when rotor speed ascends from stationary to 24000r/min with step of 2400r/min. The arrows denote speed ascending directions.

Table 1: depression effects with different f_{c1}

f_{c1} (Hz)	f_{c1} to f_{p1}	flag branch	f_1 tendency	ENV stability
1190	$f_{c1}>f_{p1}$	branch 4	$f_1<f_{p1}$, downward	unstable
1140	$f_{c1}=f_{p1}$	branch 4	$f_1<f_{p1}$, downward	stable when slower than 8400r/min
1090	$f_{c1}<f_{p1}$	branch 4→branch 2 (note 1)	$f_1<f_{p1}$, downward→ $f_1>$ f_{p1}, upward (note 1)	stable within rotational speed range
1040	$f_{c1}<<$ f_{p1}	branch 2	$f_1>f_{p1}$, upward	stable when slower than 19500r/min

Note 1：the flag branch jumps from branch 4 to branch 2 at the critical rotational speed of 15000r/min.

EXPERIMENTAL VERIFICATION

In order to verify simulation above, experiments were performed in AMB-rotor system of CMG developed by BUAA (figure 12). Relevant parameters are listed in table 2, where J_{1z} and J_{2z} are rotary inertia of axis and disk, K magnetic bearing stiffness, and ξ the damping factor respectively. Two grades of notch filters were inserted into every channel of AMB controller. Adjusting center frequency, ENV amplitudes of non-rotation suspending rotor corresponding to different f_{c1} were recorded and are showed in figure 13. The optimized f_{c1} lies in the range of from 1060 to 1120Hz, which matches simulation results very well. When f_{c1}=1095Hz, depression effect of non-rotation rotor is indicated in figure 14a, where remained ENV is at 1119Hz, lower than f_{p1}, and in -57dB, about 0.1% compared to original amplitude in figure 2. And depression effect of rotor at 10000r/min is indicated in figure 14b, where ENV frequency decreases to 1076Hz, and amplitude grows a bit to -44dB, about 1% compared to original amplitude in figure 2.

Table 2: parameters of magnetically suspended CMG

m	13.3	kg
J_{1e}	0.0138	kgm^2
J_{2e}	0.0482	kgm^2
J_{1z}	0.0014	kgm^2
J_{2z}	0.0946	kgm^2
l_m	0.06825	m
l_s	0.10275	m
k_k	540000	Nm/rad
k_v	0.8	Nms/rad
K	0.5	N/μm
ξ	0.7	----
f_{p1}	1140	Hz

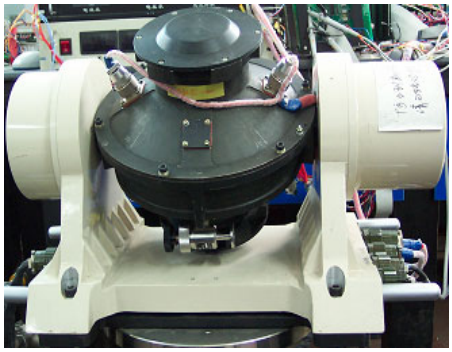

Figure 12: CMG based on magnetically suspended rotor system

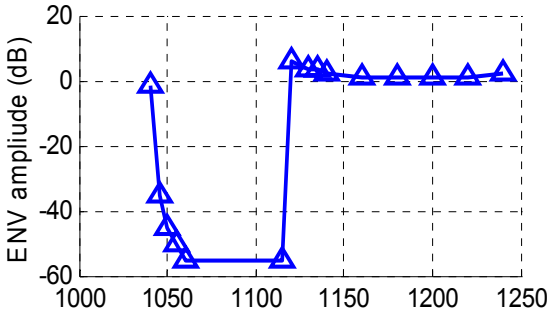

Figure 13: ENV amplitude of non-rotation suspending rotor corresponding to different center frequency of notch filter in the abscissa axis (Hz).

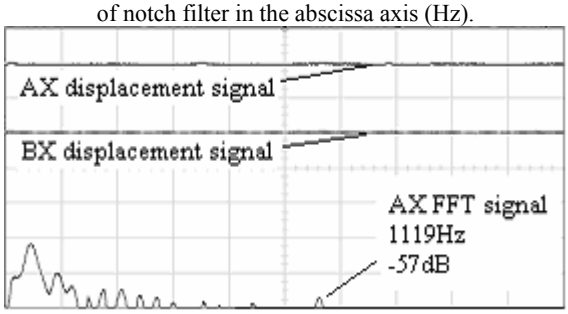

(14a) non-rotation rotor

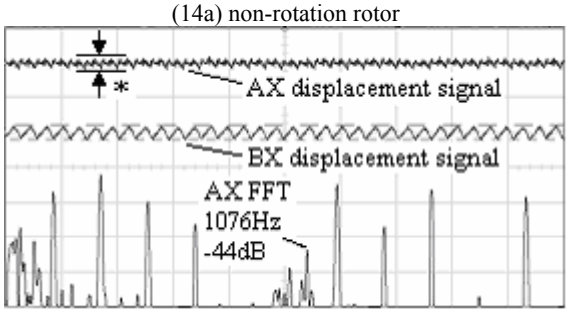

(14b) rotor at speed of 10000r/min

Figure 14: Shaft end displacement and FFT with two grades of notch filter at f_{c1}=1095Hz

Note2: The marked vibration in figure 14b results from rotor unbalance and will not be discussed here.

CONCLUSIONS

Elastic vibration mode of CMG magnetically suspended I-shaped-side-view rotor is relative bending between disk and axis which results from finite intension in conjunction. Multi-body method is adopted to model this kind of rotor considering ENV. The model introduces two new parameters, k_k and k_v, which can be evaluated by reviewing ENV frequency and stability. ENV is composed of several branches, in which flag branch with the least damping determines stability and frequency of ENV. ENV tends to be unstable with rotor speed ascending. Notch filter can be utilized to stabilize ENV. Center frequency f_{c1} is one of the most important parameters of notch filter and must be a bit lower than original frequency to obtain optimal effect of ENV suppression.

Except for center frequency, other parameters of notch filter, such as order and quality, also impact ENV depression. Base on ENV model, notch filter can be designed in general including all parameters, which will be researched in the future.

ACKNOWLEDGEMENT

The authors would like to thank Prof. Li Jichen and Dr. Zhang Liang *et al*. for their help in carrying out all the experiments.

REFERENCES

1. CMG Research Team. “Technology Report”. The 5th Unit, Beijing University of Aeronautics and Astronautics, 2002.5.
2. H. Ming Chen. “Magnetic Bearing Stiffness Control Using Frequency Band Filtering”. 1989.
3 Raoul Herzog, Philipp Buhler, Conrad Gahler and Rene Larsonneur. Unbalance Compensation Using Generalized Notch Filters in the Multivariable Feedback of Magnetic Bearing. IEEE Transactions on magnetics，1996，4(5)：580～586.
4. Lie Yu, Chongjun Yuan. (trans.) Schweitzer G., Traxler A. & Bleuler H. *Foundation, Performance and Application of Active Magnetic Bearing*. Beijing: New Era Press, 1997.
5. Kenzo Nonami and Takayuki Ito. “μ Synthesis of Flexible Rotor-Magnetic Bearing Systems”. *IEEE Transactions on magnetics*, 1996,4(5):503-512.
6. Fumitoshi Matsuno. “Vibration absorption control of force-controlled manipulators on the basis of an equivalent spring model”. *IEEE Transactions on industrial electronics*, 1995,42(5):501-505.
7. Gianni Ferretti, GianAntonio Magnani and Paolo Rocco. “2002 Modeling and experimental analysis of the vibrations in hard disk drives”. *IEEE/ASME Transactions on mechatronics*, 2002,7(2):152-160.
8. D. Fermental, E. Cusson and P. Larocca. “A Decomposition of The Jeffcott Rotor”. *The 2nd International Symposium on Magnetic Bearing*, 1990:289-294.
9. P.Larocca, D.Fermental and E.Cusson. “Performance Comparison between Centralized and Decentralized Control of the Jeffcott Rotor”. *The 2nd International Symposium on Magnetic Bearing*, 1990:295-300.